PHYSICAL REVIEW A VOLUME 36, NUMBER 6 SEPTEMBER 15, 1987

Autoionization in a strong laser field with variable laser band shape

Z. Deng* and J. H. Eberly
Department of Physics and Astronomy, University of Rochester, Rochester, New York 14627
(Received 22 October 1986)

We present a theoretical study of strong-field autoionization electron spectra, including laser dephasing with variable band shape. We show that in the weak-field limit the usual peak reversal is obtained when the spectrum changes from the Lorentzian limit to the Gaussian limit. When the laser field strength is increased, different peak reversal behaviors are predicted in the Lorentzian and Gaussian limits, which is quite different from that in the weak-field case. A comparison between the effect of Doppler and laser dephasing on the photoelectron spectrum of autoionization is also made in the static limit.

I. INTRODUCTION

Since the discussion of autoionization by Fano,[1] the photoelectron and photon emission spectra of laser-induced autoionization have been intensively studied,[2–9] especially for the strong-field effects of autoionization.[10–16] Several remarkable coherent effects, including the Fano zero[1] and the confluence,[10] are now well understood. In real experiments these coherent effects will be affected by line-broadening processes, such as spontaneous emission, the Doppler effect, collisions, and laser dephasing. These incoherent effects help to determine the autoionization photoelectron spectrum and have been studied by several authors.[17–22]

In some recent studies of laser-induced autoionization with dephasing processes, the common constant dephasing relaxation coefficients were introduced into the Bloch equations, and this corresponds to the case when the correlation time of the dephasing process is short.[11,17] It was shown that the Fano zero is still present, but the confluence is destroyed completely with the presence of the dephasing process.

The effect of different band shapes on the autoionization spectrum in the weak-field case was studied recently.[21] It was shown that the usual peak reversal can be found in the autoionization spectrum. That is, in the Lorentzian band-shape limit the inelastic peak is higher than the elastic peak and in the Gaussian band-shape limit the inelastic peak is lower than the elastic peak. The question is, do we find the same kind of peak reversal in the strong-field case?

We now consider a strong-field autoionization model in which the laser dephasing is described by a Gaussian-Markov process and its band width is finite. We show that the long-time photoelectron spectrum can be expressed in terms of an infinite matrix continued fraction. The spectra in various cases are studied, and we show that the peak reversals and the photoelectron line shapes in weak- and strong-field cases are quite different. We show that the elastic peak decreases in the Lorentzian limit but increases in the Gaussian limit as the laser field increases. This is due to the total effects of the ac Stark splitting, the laser dephasing, and the autoionization mixing. We also show that the effect of the Doppler broadening and the laser dephasing are different. For example the Fano zero will be destroyed by the Doppler broadening but not by the laser dephasing.

In Sec. II we describe the Hamiltonian of our model. The phase of the laser obeys a Gaussian-Markovian process, and its properties are determined by two parameters. Adjustment of these parameters allows both the bandwidth and the band shape of the laser to be changed. In Sec. III we show that by using the assumption of a flat continuum, we can transform the original stochastic integrodifferential equations into a set of stochastic differential equations. This procedure enables us to solve the model by using well-established techniques, and the photoelectron spectrum is expressed in terms of an infinite continued fraction.

In Sec. IV we study the simplest case. That is, the model only contains one discrete state and a continuum. The purpose of this section is to show explicitly that in the static limit, we can simply treat the random variable as a constant. After solving the entire problem, the spectrum is averaged over the random variable with a certain distribution function. We then compare this with Doppler broadening. We show that even though the method to solve these two processes, i.e., the dephasing process in the static limit and the Doppler broadening, are the same, in general different results will be obtained since the physical origins of these two processes are different.

In Sec. V we present some numerical analysis of the result obtained in Sec. III. The spectrum is compared in the Gaussian and Lorentzian limits. We show different peak reversal behaviors in the weak- and strong-field cases. Finally, some conclusions are made in Sec. VI.

II. DESCRIPTION OF MODEL

We consider the autoionization model shown in Fig. 1. The figure shows a bound state in one electronic configuration, labeled $|1\rangle$, which is mixed by a Coulombic interaction with the continuum of another configuration, labeled $|\omega\rangle$, leading to the creation of an autoionizing resonance. An initially occupied ground

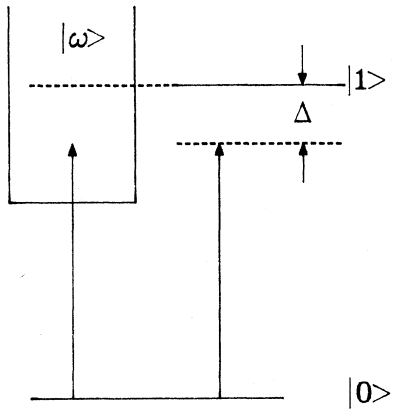

FIG. 1. Simplified atomic level scheme and detuning for our autoionization model.

state $|0\rangle$ is coupled to these states through an induced-dipole transition by a laser with frequency ω_L. The model assumes that the laser phase is described by a stochastic variable $\phi(t)$. The total Hamiltonian for our system, within the rotating-wave approximation (RWA) is given by (with $\hbar=1$)

$$H=H_0+V_1+V_2 , \tag{1}$$

where

$$H_0=\Delta|1\rangle\langle 1|+\int d\omega\omega|\omega\rangle\langle\omega| \tag{2}$$

and

$$V_1=\frac{\Omega}{2}|0\rangle\langle 1|e^{i\phi(t)}+\int d\omega D_{0\omega}|0\rangle\langle\omega|e^{i\phi(t)}+\text{H.c.} , \tag{3}$$

$$V_2=\int d\omega D_{1\omega}|1\rangle\langle\omega|+\text{H.c.} . \tag{4}$$

Here $E_1\equiv\Delta=\omega_{10}-\omega_L$ is the detuning, and ω is the energy of the continuum measured from the energy where the laser is tuned. V_1 specifies laser-induced dipole interactions and V_2 is for the Coulombic interaction. Since we assume that the continuum is flat, $D_{0\omega}$ and $D_{1\omega}$ are independent of ω.

From the single-mode model of laser theory we know that if a single-mode laser is far above threshold, its phase $\phi(t)$ is governed by the following stochastic equation:[7,23]

$$\dot{\chi}+\beta\chi=F(t) , \tag{5}$$

where

$$\chi\equiv\frac{d\phi}{dt} , \tag{6}$$

and $F(t)$ is a δ-correlated Gaussian force fulfilling[24]

$$\langle F(t_1)F(t_2)\rangle=2b\beta^2\delta(t_1-t_2) . \tag{7}$$

This random process has such a property that

$$\langle\chi(t_1)\chi(t_2)\rangle=b\beta e^{-\beta|t_1-t_2|} . \tag{8}$$

The properties of the phase fluctuation are therefore determined by two parameters β and b, and $1/\beta$ is the correlation time of $\chi(t)$.

In the limit $\beta\to\infty$, $\chi(t)$ becomes δ correlated and ϕ can be described by the Wiener-Levy process.[25] We know that dynamic equations with such a random process can be solved exactly.[26] It is equivalent to introduce a constant dephasing coefficient into the dynamic equations. The detailed analysis of the electron and photon spectra of the different autoionization models have been studied in this limit.[11,17] But for finite β this procedure breaks down. We cannot, in general, solve the problem exactly. As we shall show, the long-time photoelectron spectrum can be expressed in terms of a matrix continued fraction.

With the total Hamiltonian given by Eq. (1), we can get the dynamic equations of the system. Usually before doing so, a diagonalization of the partial Hamiltonian H_0+V_2 is accomplished to get the Fano states. The problem is then solved in the diagonalized new space. This procedure will usually end up with some integrodifferential equations. It is difficult to solve the model involving a dephasing process with finite β. We will not follow this procedure in the present discussion. In Sec. III we shall use the total Hamiltonian to get the dynamic equations of motion directly. We show that by the assumption of flat continuum, the integrodifferential equation can be transformed into a set of differential equations, and the usual way[27] to solve the stochastic equations with finite β can be applied.

III. EQUATIONS OF MOTION AND LONG-TIME PHOTOELECTRON SPECTRUM

In this section we use the total Hamiltonian given by Eq. (1) to get the equations of motion. They are integrodifferential equations with the random variable $\chi(t)$ subject to Eq. (5). We first show that these integrodifferential equations can be transformed to differential equations by using the assumption of a flat continuum. This procedure allows us to apply the standard method we have introduced to get a set of averaged equations. Then the photoelectron spectrum is expressed by a matrix continued fraction.

In the Schrödinger picture the exact state function can be written as

$$|\psi(t)\rangle=\alpha_0(t)|0\rangle+\alpha_1(t)|1\rangle+\int d\omega\alpha_\omega(t)|\omega\rangle . \tag{9}$$

By using the Schrödinger equation we can obtain the following Bloch-type equations of motion (in the rotating frame)

$$\dot{C}_{00}=-i\frac{\Omega_0}{2}C_{01}-i\int d\omega D_{0\omega}C_{0\omega}+\text{c.c.} , \tag{10a}$$

$$\dot{C}_{11}=-i\frac{\Omega_0^*}{2}C_{10}-i\int d\omega D_{1\omega}C_{1\omega}+\text{c.c.} , \tag{10b}$$

$$\dot{C}_{01}=-i(\Delta-\chi)C_{01}+i\frac{\Omega_0^*}{2}(C_{11}-C_{00}) -i\int d\omega D_{0\omega}C_{0\omega}+i\int d\omega D_{0\omega}C_{\omega 1} , \tag{10c}$$

$$\dot{C}_{0\omega}=-i(\omega-\chi)C_{0\omega}-iD_{\omega 0}C_{00}-iD_{\omega 1}C_{01}+i\frac{\Omega_0^*}{2}C_{1\omega}+i\int d\omega' D_{\omega 0}C_{\omega'\omega}\ , \tag{10d}$$

$$\dot{C}_{1\omega}=-i(\omega-\Delta)C_{1\omega}+i\frac{\Omega_0^*}{2}C_{0\omega}-iD_{\omega 0}C_{10}-iD_{\omega 1}C_{11}+i\int d\omega' D_{\omega 1}C_{\omega'\omega}\ , \tag{10e}$$

$$\dot{C}_{\omega\omega'}=-i(\omega'-\omega)C_{\omega\omega'}+iD_{0\omega}C_{0\omega'}-iD_{\omega 0}C_{\omega 0}+iD_{1\omega}C_{1\omega'}-iD_{\omega 1}C_{\omega' 1}\ , \tag{10f}$$

where χ is defined in Eq. (5), and we have introduced the new variables

$$C_{lk}=\alpha_l^*\alpha_k,\quad l,k=0,1,\omega,\omega'\ , \tag{11}$$

except

$$C_{01}=C_{10}^*=\alpha_0^*\alpha_1 e^{i\phi(t)}\ , \tag{12a}$$

$$C_{0\omega}=C_{\omega 0}^*=\alpha_0^*\alpha_\omega e^{i\phi(t)}\ . \tag{12b}$$

These integrodifferential equations must be solved with the initial condition

$$C_{00}(0)=1\ . \tag{13}$$

We cannot directly use the Laplace transformation to solve this problem, because these equations are also stochastic equations with the time-dependent random variable $\chi(t)$.

Since the continuum is assumed to be flat, it has been shown that the integrodifferential equations can be transformed into differential equations:[21]

$$\left[\frac{d}{dt}+A+i\chi(t)B\right]\psi(t)=0\ . \tag{14}$$

Here A and B are all matrices given by

$$A=\begin{bmatrix}A_1 & 0\\ A_2 & A_3\end{bmatrix} \tag{15}$$

and

$$A_1=\begin{bmatrix}2\gamma_{00} & 0 & \mu_1 & \mu_1^*\\ 0 & 2\gamma_{11} & \mu_2 & \mu_2^*\\ \mu_2^* & \mu_1^* & (\gamma_{00}+\gamma_{11})+i\Delta & 0\\ \mu_2 & \mu_1 & 0 & (\gamma_{00}+\gamma_{11})-i\Delta\end{bmatrix}, \tag{16a}$$

$$A_2=\begin{bmatrix}iD_{\omega 0} & 0 & iD_{\omega 1} & 0\\ 0 & iD_{\omega 1} & 0 & iD_{\omega 0}\end{bmatrix}, \tag{16b}$$

$$A_3=\begin{bmatrix}i\omega+\gamma_{00} & \mu_1^*\\ \mu_2 & i(\omega-\Delta)+\gamma_{11}\end{bmatrix}, \tag{16c}$$

where

$$\mu_1=\frac{i}{2}\Omega_1+\gamma_{01}\ , \tag{17a}$$

$$\mu_2=-\frac{i}{2}\Omega_0+\gamma_{01}\ . \tag{17b}$$

The elements of the matrix B are given by

$$B_{ij}=0\ , \tag{18}$$

except

$$B_{33}=-B_{44}=B_{55}=1\ . \tag{19}$$

$\psi(t)$ represents the atomic variable given in the order of C_{00}, C_{11}, C_{01}, C_{10}, $C_{0\omega}$, and $C_{1\omega}$. In Eqs. (16) $\gamma_{\alpha\beta}$ is due to the discrete-continuum coupling given by

$$\gamma_{\alpha\beta}=\pi D_{\alpha\omega}D_{\omega\beta}^*\ . \tag{20}$$

From Eq. (15) we notice that the total atomic space is divided into three subspaces. The first subspace 00,11,01,10 is self-contained. The second subspace $0\omega,\omega 0,1\omega,\omega 1$ only couples to the first subspace, and the third subspace $\omega\omega$ only couples to the second, but not vice versa. Still we notice that Eq. (14) is a stochastic differential equation.

What we are interested in is the averaged long-time photoelectron spectrum. As we know, the long-time photoelectron spectrum can be given by

$$W(\omega)=\langle\tilde{C}_{\omega\omega}(z=0)\rangle\ , \tag{21}$$

and more explicitly we have

$$W(\omega)=\mathrm{Im}[D_{0\omega}\langle\tilde{C}_{0\omega}(z=0)\rangle+D_{1\omega}\langle\tilde{C}_{1\omega}(z=0)\rangle]\ , \tag{22}$$

where the average is with respect to the random variable $\chi(t)$ and $\tilde{C}_{\alpha\beta}(z)$ is the Laplace transformation of $C_{\alpha\beta}(t)$. So if we can find the averaged quantities $\langle\tilde{C}_{0\omega}\rangle$ and $\langle\tilde{C}_{1\omega}\rangle$ from Eq. (14), we can then substitute them into Eq. (22) to get the photoelectron spectrum.

A type of the stochastic equation given by Eq. (14) with the random variable $\chi(t)$ obeying Eq. (5) is well studied.[25,27] Following the same procedure we have

$$\tilde{\psi}(z)=\frac{1}{z+A+\hat{K}(z)}\psi(0)\ , \tag{23}$$

where $\hat{K}(z)$ is the matrix continued fraction

$$\hat{K}(z)=B\cfrac{\beta b}{z+\beta+A+B\cfrac{2\beta b}{z+2\beta+A+\cdots}}B\ , \tag{24}$$

Here $\tilde{\psi}(z)$ is the Laplace transformation of $\psi(t)$. The dynamics of the system can be obtained by inverting the Laplace transformation of Eq. (23). Since now we only want to know the spectrum in the long-time limit, we simply let $z=0$ in Eq. (23) to get averaged $\langle\tilde{C}_{0\omega}\rangle$ and $\langle\tilde{C}_{\omega 0}\rangle$. The photoelectron spectrum is then given by Eq. (22).

Equations (22) and (23) are our main result and shall be studied in the following sections. By truncating the matrix continued fraction at some finite level (including enough levels till the result converged), we can study the effect of the dephasing in the spectrum, especially with finite correlation time.

IV. STATIC LIMIT AND DOPPLER BROADENING

In Sec. III we have solved the stochatsic differential equations, and the long-time photoelectron spectrum was expressed in terms of a matrix continued fraction.

This procedure is valid for any correlation of the laser dephasing. This method is quite general, but somewhat complicated. We then ask whether we can find some simple way to solve it. For example, is it possible that we simply solve the model by regarding the random variable $\chi(t)$ as a constant parameter, and then averaging the result with respect to the distribution of $\chi(t)$. As we know, since the distribution function of the random variable is time dependent, in general we cannot follow this procedure. Only in the static limit given by

$$\beta \to 0 , \tag{25a}$$

$$\beta b \to \Gamma^2 , \tag{25b}$$

where Γ is a constant, does the distribution function of the random variable become time independent. Then the simple procedure can be applied.

In this section we first solve a simple model by using the method we have used in Sec. III. Then we solve the same model in a way that the random variable is treated as a constant parameter, and after solving the problem we perform the average. We show explicitly that in the static limit, the two procedures give the same result. We also show that even though the second method is similar to the method used by Haus *et al.* recently to study Doppler broadening effects on the autoionizing spectrum,[20] in general the two processes will give different results. This is because the variables to be averaged are different. Only in some special cases the same result can be obtained.

To make things more transparent, we assume that the model only contains a ground state $|0\rangle$ and a flat continuum $|\omega\rangle$. This is equivalent to say that

$$\Omega_0 = D_{1\omega} = 0 \tag{26}$$

in our autoionization model introduced in Sec. II. From Eq. (16) we know that in this case A and B become 2×2 matrices given by

$$A = \begin{bmatrix} 2\gamma_{00} & 0 \\ \frac{i}{2}\Omega_0 & i\omega+\gamma_{00} \end{bmatrix} , \tag{27}$$

$$B = \begin{bmatrix} 0 & 0 \\ 0 & 1 \end{bmatrix} , \tag{28}$$

with $\psi=(C_{00}, C_{0\omega})$. By substituting matrices A and B into Eq. (23), it is easy to show that $\tilde{C}_{0\omega}$ can be expressed in terms of a number continued fraction:

$$\langle \tilde{C}_{0\omega} \rangle = \frac{-i\Omega_0}{(z+\gamma_{00})(z+i\omega+\gamma_{00}+G_0)} , \tag{29}$$

where

$$G_0 = \cfrac{\beta b}{z+\beta+i\omega+\gamma_{00}+\cfrac{2\beta b}{z+2\beta+i\omega+i\omega+\gamma_{00}+\cdots}} . \tag{30}$$

To compare with this result, we solve the problem alternatively. This time we regard χ in Eq. (14) as a constant, and by solving Eq. (14) with A and B given by Eq. (27) and Eq. (28) we simply get

$$\tilde{C}_{0\omega} = \frac{-i\Omega_0}{(z+\gamma_{00})(z+i\omega+\gamma_{00}+i\chi)} . \tag{31}$$

In the static limit the time-independent distribution function of χ is a Gaussian function:

$$P(\chi) = (2\pi\Gamma^2)^{-1} e^{-\chi^2/(2\Gamma^2)} . \tag{32}$$

By averaging Eq. (31) with this distribution function we have

$$\langle \tilde{C}_{0\omega} \rangle = \int_{-\infty}^{\infty} d\chi\, P(\chi) \tilde{C}_{0\omega} = \cfrac{-i\Omega_0/(z+\gamma_{00})}{z+i\omega+\gamma_{00}+\cfrac{\Gamma^2}{z+i\omega+\gamma_{00}+\cfrac{2\Gamma^2}{z+i\omega+\gamma_{00}+\cdots}}} . \tag{33}$$

It is clear that if we take the static limit given by Eqs. (25), Eq. (30) and Eq. (33) are identical.

Physically the static limit means that the coherence time of the stochastic process $\tau_c = 1/\beta$ is long compared with the time interval which characterizes the dynamics of the system, such as $1/\Omega_0$. Within this time regime, we can simply treat the random variable as a constant. After solving the problem we should take the ensemble average. This procedure is no longer valid if the coherence time τ_c is not longer than the time interval in which the electron is ionized. In this case the random variable can change its values during this period of time and we have to solve the entire stochastic equations as we have done in Sec. III.

As far as Doppler broadening is concerned, we should average the spectrum with respect to ω in Eq. (31) instead of χ. This is because in an atomic ensemble, atoms move with different velocities. What are measured are the outgoing electrons with the sum of the ionization energy and the kinetic energy of the moving atoms. We have to average the energy of the outgoing electrons with respect to the ensemble of the moving atoms. Since the variables to be averaged are different, the two processes, the Doppler broadening and the laser dephasing in the static limit, will, in general, give different results. This can be seen from Eqs. (10) where the positions of χ and ω are different [for example, in Eq. (10c) there is no ω but χ].

For the present simple case, let $\chi=0$ in Eq. (31) and take the average over ω with the Doppler distribution function given by

$$P(\omega) = (2\pi\Gamma^2)^{-1} e^{-(\omega-\bar{\omega})^2/(2\Gamma^2)} , \tag{34}$$

where $\bar{\omega}$ is the value for the stationary atoms. Again we get the same expression as Eq. (33) simply replacing ω by $\bar{\omega}$. For this simple model the two processes give the same result, because ω and χ in Eq. (31) are exactly in the same position. But in general they are different. For example in the Fano model, as we shall discuss in Sec. V, the Doppler broadening destroys the Fano zero com-

pletely, but for the dephasing broadening we always have the Fano zero in the electron spectrum.

V. NUMERICAL RESULTS AND DISCUSSION

In Sec. III we have expressed the long-time photoelectron spectrum in terms of the matrix continued fraction which is valid for any β. As we know, the stochastic properties of the laser field are determined by β and b. More explicitly the spectrum of the laser described by Eq. (5) is given by the Fourier transform of the correlation function

$$\langle e^{i\phi(t+\tau)-i\phi(\tau)}\rangle = \exp\{-b[\,|\tau|+(e^{-\beta|\tau|}-1)/\beta]\}\ . \tag{35}$$

For $b<\beta$ the spectrum of the laser is Lorentzian with the effective width b. We call this the Lorentzian limit. In the static limit given by Eq. (25) the laser spectrum becomes Gaussian with effective width Γ. For this reason we refer it as the Gaussian limit. The line shape of the photoelectron spectrum is therefore significantly influenced by the values of β and b.

In the static or Gaussian limit, since the distribution function of $\chi=\dot{\phi}$ is independent of time, one can solve the problem of regarding χ as a constant and take the stochastic average after solving the problem as we did in Sec. IV. If we substitute the static limit given by Eqs. (25) into Eq. (24), we shall get the same type of equation as Eq. (33) but in a matrix form. The advantage of Eq. (24) is that it holds for any finite numbers b and β.

For further discussion, we introduce an asymmetry parameter

$$q \equiv \frac{\Omega_0}{2(\pi\gamma_{11})^{1/2}D_{0\omega}}\ , \tag{36}$$

which specifies the ratio of the direct and indirect ionization channels. Here γ_{11} specifies the decay rate of the level $|1\rangle$ due to the Coulombic interaction. To compare the spectrum in the Gaussian and Lorentzian limits, in the following calculations we choose $\beta=125$, $b=5$ for the Lorentzian limit, and $\beta=1$, $b=25$ for the Gaussian limit, so that the same effective width ($=5$) is obtained for both cases.

The spectrum in the Lorentzian limit is simple. From Eq. (23) we have

$$\tilde{\psi}(z)=\frac{1}{z+A+bB^2}\psi(0)\ . \tag{37}$$

The effect of the laser dephasing can be described by introducing a constant dephasing coefficient b which is clearly shown in Eq. (37). The detailed properties of the spectrum have been studied by Rzążewski and Eberly.[11] They showed that the presence of incoherent dephasing does not eliminate the Fano zero in the spectrum. This is because the effect of dipole phase diffusion is exactly the same on both of the two ionization channels and so they do not accumulate any relative phase mismatch. On the other hand, however, the confluence will be destroyed completely by incoherent dephasing since there is an absolute effect on dipole coherence and, as a consequence, Autler-Townes interference is weakened. This is shown in Fig. 2 where the Fano zero is located at $\omega=\gamma_{11}q=3$ since $\gamma_{11}=1$ and $q=3$. In Fig. 2 the dashed line is plotted for $\Gamma=1$ and the solid line is for $\Gamma=10$.

If q is very large, the direct transition channel is negligible. The problem is similar to studying the absorption spectrum of the probe field in double optical resonance discussed by Dixit *et al.*[27] In this case they showed the different aspects of the absorption line shape in the Gaussian and Lorentzian limits and they found that in the Lorentzian limit the inelastic peak is higher than the elastic peak but in the Gaussian limit the elastic peak is higher than the inelastic peak. This is called peak reversal. In the following discussions we show that the same peak reversal can be seen in the weak field case but not in the strong field case since q is taken to be finite.

When q takes some finite value, the coherent interference of two ionization channels will enter the picture. In Fig. 3 we have chosen $\Delta=30$ and $\Omega_0=1$, so it is the spectrum in the weak field case. In this figure the zero appears at $\omega=25$ since we assume $\gamma_{11}=1$, $q=25$ and therefore $\omega=\gamma_{11}\,q=25$. In Fig. 3 the peak heights are quite different in the Lorentzian and Gaussian limits. In the Lorentzian limit the inelastic peak is higher than the elastic peak. On the other hand, in the Gaussian limit the inelastic peak is lower than the elastic peak. This is because the laser spectrum in the Lorentzian and Gaussian limits are Lorentzian and Gaussian, respectively. As we know, the Gaussian spectrum drops much faster than that of the Lorentzian spectrum, especially in the far wing region. Physically the peak reversal is caused by the overlap of the wing of the dephasing broadening with the atomic resonance. If the detuning is large, the smaller overlap of the laser dephasing broadening with

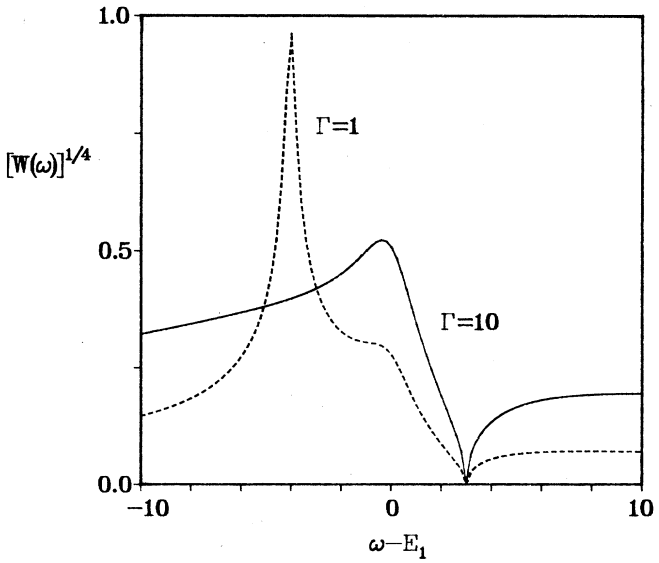

FIG. 2. Long-time photoelectron spectrum with parameters $\Omega_0=1$, $q=3$, $\Delta=4$, and $\gamma_{11}=1$ ($E_1=\Delta$). Solid line is drawn with $\Gamma=10$, and dashed line is for $\Gamma=1$.

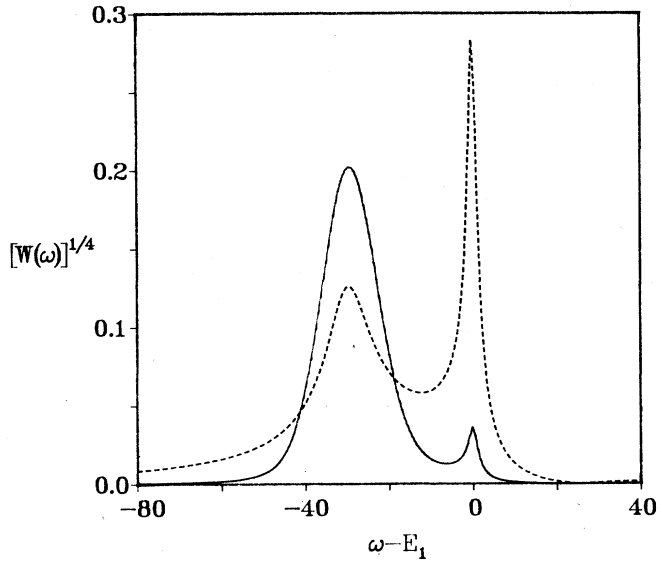

FIG. 3. Long-time photoelectron spectrum with parameters $q=25$, $\Delta=30$, $\gamma_{11}=1$, and $\Omega_0=1$ ($E_1=\Delta$). Solid line is drawn for the Gaussian limit with $\beta=1$ and $b=25$, and dashed line is for the Lorentzian limit with $\beta=125$ and $b=5$.

the atomic resonance in the Gaussian limit leads to a decrease of the indirect transition channel which results a decrease of the inelastic peak.

If the laser field is increased, as shown in Figs. 4 and 5 where $\Omega_0=30$ and 50, respectively, we observe a new kind of peak reversal. Figure 4 is plotted for $\Omega_0=30$. In this case the spectrum in the two limits are quite similar. When the Rabi frequency increases to 50 as shown in Fig. 5, the peak close to the Fano zero in the Gaussian limit gets much higher than in the Lorentzian limit. What we have observed from these is that one of the ac Stark peaks in the Gaussian limit is getting higher and higher, as it is moving close to the Fano zero. In

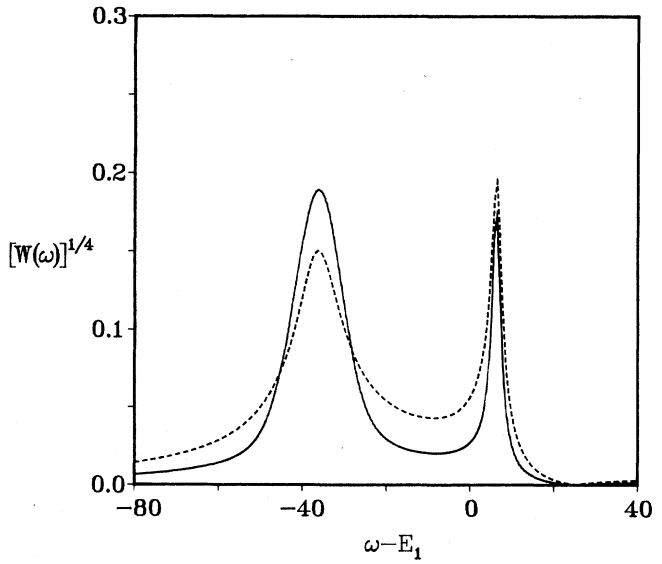

FIG. 4. The same as in Fig. 3 except $\Omega_0=30$.

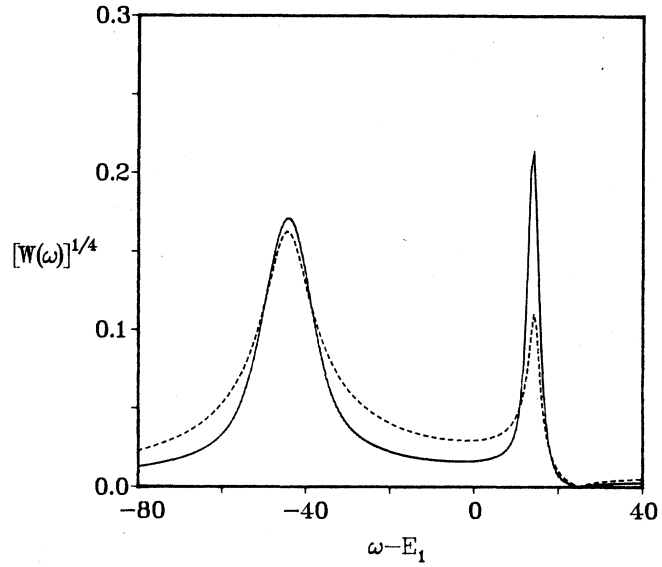

FIG. 5. The same as in Fig. 3 except $\Omega_0=50$.

the Lorentzian limit, however, the same peak gets lower as we increase the laser power. This new kind of peak reversal is laser-power dependent. This is the new feature in our model. It indicates that the coherent interference of the two ionization channels is important to determine the difference of the spectrum in the two limits.

If the field is weak and the detuning is large, the elastic peak in the Gaussian limit is higher than in the Lorentzian limit, and the inelastic peak in the Gaussian limit is lower than in the Lorentzian limit. This kind of peak reversal is caused by the different overlap of the wing of the laser spectrum with the atomic resonance in the Gaussian and Lorentzian limits. To understand the physical origin of the new peak reversal phenomenon in the strong field case, let us first consider the spectrum in the Gaussian limit where the peak close to the Fano zero becomes higher when the laser field increases. As we mentioned before, we can solve the problem in the Gaussian limit by referring the random variable χ as a constant parameter and then average the result with respect to the distribution of χ. By taking $\chi=0$ the behavior of the autoionization spectrum reduces to the case without any random dephasing process.[10] In this case, one of the ac Stark peaks gets higher as it gets closer to the Fano zero due to the confluence effect. It can be shown that when $\chi\neq 0$ we still can see that the confluence effect plays a role. Therefore it is the confluence effect which makes the peaks close to the Fano zero get higher in the Gaussian limit as we increase the laser field. In the Lorentzian limit, however, the confluence will be destroyed by the dephasing process.[11] Also in the Lorentzian limit the peak close to the Fano zero will be broadened by the dephasing process as we increase the laser field due to the mixing of the levels $|0\rangle$ and $|1\rangle$ (in the weak-field case the inelastic peak is only broadened by the decay rate γ_{11}). For these reasons the peak close to the Fano zero gets lower when the laser field is increased.

If q is finite in our model we always have the Fano zero in the photoelectron spectrum. This is true in any limits, including the static limit we have discussed in Sec. IV. This is quite different from Doppler type of broadening. As discussed by Haus *et al.*, the Doppler broadening destroys the Fano zero completely.[20] The appearance of the Fano zero in our model is due to the two ionization channels not accumulating any relative phase mismatch. But in the Doppler broadening the ensemble average over the random motion of the atoms washes out all the coherent effects. This case serves as an example for the different results obtained from the Doppler broadening and laser dephasing broadening in the static limit.

Recently Rzążewski and Cooper[22] considered the effect of a fluctuating electronic field due to the surrounding plasma environment. The main effect caused by this fluctuating electric field is dipole transitions from the imbedded ionization state to a set of neighboring states of the opposite parity. In the weak-field limit, the ionization rate was derived in both the short correlation time of the fluctuating electric field (dilute plasma) and the finite bandwidth fluctuating electric field case (dense plasma). The fluctuating electric field gives an additional width and shift to the line shape of the ionization rate as a function of the laser detuning. Our work differs from theirs as follows. (1) In our case the phase of the laser field is a random variable, while in their case it is the electric field due to the surrounding plasma environment that is fluctuating. (2) We have studied the photoelectron spectrum in the weak- and strong-field cases, but they limited themselves to the weak-field case and only the ionization rate was studied. (3) We have specially shown the different peak reversals and line shapes in the weak- and strong-field cases. In addition, the difference between the Doppler broadening and the laser dephasing has been studied.

VI. CONCLUSION

We have studied an autoionization model including laser dephasing with a variable band shape. The laser dephasing is described by a Gaussian-Markov process and its bandwidth is finite. By using the standard method, the long-time photoelectron spectrum has been expressed in terms of an infinite matrix continued fraction and has been studied in various cases.

We have shown explicitly that in the static limit the problem can be solved by a simple method in which the random variable is treated as a constant parameter, and after solving the problem we perform the stochastic average. We have compared the spectrum in the static limit with the autoionization spectrum including the Doppler broadening recently studied by Haus *et al.* and have shown that the effects of the Doppler broadening and the laser dephasing are different. For example, in our model we always have the Fano zero on the photoelectron spectrum. But the Doppler broadening, as discussed by Haus *et al.* destroys the Fano zero completely.

The focusing point of the present discussion is to show the different aspects of the photoelectron spectrum in the strong field as the laser dephasing changing from the Lorentzian limit to the Gaussian limit. In the weak-field limit, the usual peak reversal can be seen, i.e., in the Lorentzian limit the inelastic peak is higher than the elastic peak, but in the Gaussian limit the elastic peak is higher than the inelastic peak. But when the laser power is increased, a different kind of peak reversal is predicted. We have shown that as the laser power is increased, the inelastic peak decreases in the Lorentzian limit but increases in the Gaussian limit. Therefore, the line shapes in the strong-field case are quite different from that in the weak-field case. This is due to the fact that in the Lorentzian limit the dephasing process destroys the confluence effect completely but not in the Gaussian limit.

ACKNOWLEDGMENT

This work was supported by the U.S. Office of Naval Research and by the U.S. Air Force Office of Scientific Research.

*Present address: Institute of Optics, University of Rochester, Rochester, NY 14627.

[1]U. Fano, Phys. Rev. **124**, 1866 (1961).
[2]L. Armstrong, Jr., B. L. Beers, and S. Feneuille, Phys. Rev. A **12**, 4637 (1975).
[3]Yu I. Heller and A. K. Popov, Opt. Commun. **18**, 449 (1976).
[4]L. Armstrong, Jr., C. E. Theodosiou, and M. J. Wall, Phys. Rev. A **18**, 2538 (1978).
[5]A. T. Georges and P. Lambropoulos, Phys. Rev. A **18**, 587 (1978).
[6]P. L. Knight, J. Phys. B **12**, 3297 (1979); *Laser Physics,* edited by D. F. Walls and J. Harvey (Academic, Sydney, 1980).
[7]P. Lambropoulos and P. Zoller, Phys. Rev. A **24**, 379 (1981).
[8]P. E. Coleman and P. L. Knight, J. Phys. B **14**, 2139 (1981).
[9]Yu I. Heller, V. F. Lukinykh, A. K. Popov, and V. V. Slabko, Phys. Lett. **82A**, 4 (1981).
[10]K. Rzążewski and J. H. Eberly, Phys. Rev. Lett. **47**, 408 (1981).
[11]K. Rzążewski and J. H. Eberly, Phys. Rev. A **27**, 2026 (1983).
[12]J. H. Eberly, K. Rzążewski, and D. Agassi, Phys. Rev. Lett. **49**, 693 (1982).
[13]M. Crance and L. Armstrong, Jr., J. Phys. B **15**, 4637 (1982).
[14]A. Lami and N. K. Rahman, Opt. Commun. **43**, 383 (1982); Phys. Rev. A **26**, 3360 (1982); **33**, 782 (1986).
[15]Z. Bialynicka-Birula, Phys. Rev. A **28**, 836 (1983).
[16]Z. Deng and J. H. Eberly, J. Opt. Soc. Am. B **1**, 102 (1983).
[17]G. S. Agarwal, S. L. Haan, K. Burnett, and J. Cooper, Phys. Rev. Lett. **48**, 1164 (1982); Phys. Rev. A **26**, 2277 (1982).
[18]G. S. Agarwal and D. Agassi, Phys. Rev. A **27**, 2254 (1983).
[19]M. Lewenstein, J. W. Haus, and K. Rzążewski, Phys. Rev. Lett. **48**, 1164 (1983); J. W. Haus, M. Lewenstein, and K.

Rzążewski, Phys. Rev. A **28**, 2269 (1983).
[20]J. W. Haus, K. Rzążewski, and J. H. Eberly, Opt. Commun. **46**, 191 (1983).
[21]Z. Deng, J. Phys. B **18**, 2387 (1985).
[22]K. Rzążewski and J. Cooper (unpublished).
[23]H. Haken, in *Handbuch der Physik,* edited by S. Flugge (Springer, Berlin, 1970), Vol. XXV/2c.
[24]M. C. Wang and G. E. Uhlenbeck, Rev. Mod. Phys. **17**, 323 (1945).
[25]K. Wódkiewicz, J. Math. Phys. **20**, 45 (1979); **23**, 2179 (1982).
[26]R. Fox, J. Math. Phys. **13**, 1196 (1972).
[27]S. N. Dixit, P. Zoller, and P. Lambropoulos, Phys. Rev. A **21**, 1289 (1980).